Phytochemistry 163 (2019) 23–32

Contents lists available at ScienceDirect

Phytochemistry

journal homepage: www.elsevier.com/locate/phytochem

Anti-inflammatory terpenes from *Schefflera rubriflora* C. J. Tseng & G. Hoo with their TNF-α and IL-6 inhibitory activities

Fenghua Li[a], Jian Zhang[b], Mingbao Lin[a], Xianming Su[a], Changkang Li[a], Hongqing Wang[a], Baoming Li[a], Ruoyun Chen[a], Jie Kang[a,*]

[a] State Key Laboratory of Bioactive Substances and Functions of Natural Medicines, Institute of Materia Medica, Chinese Academy of Medical Sciences & Peking Union Medical College, No. 1 Xiannongtan Street, Beijing 100050, China
[b] Department of Bioengineering, Zhuhai Campus of Zunyi Medical University, Zhuhai 519041, China

ARTICLE INFO

Keywords:
Schefflera rubriflora C. J. Tseng & G. Hoo
Araliaceae
Terpene
Anti-inflammatory activity
TNF-α
IL-6

ABSTRACT

The 95% ethanol extract and its EtOAc and *n*-BuOH fractions obtained from the leaves and twigs of *Schefflera rubriflora* C. J. Tseng & G. Hoo showed significant inhibitory activities (33.6%, 35.7% and 40.6%, respectively) against croton oil-induced ear inflammation in mice. Bioactivity-guided isolation and separation gave eight previously undescribed terpenes or terpene glycosides. Structural elucidation was based on UV, IR, and NMR spectroscopy, MS, experimental and calculated ECD data, and Mosher's method. To identify anti-inflammatory components from the extract, all the compounds were evaluated for tumor necrosis factor-α (TNF-α) and interleukine-6 (IL-6) inhibitory activities. Four undescribed compounds inhibited mRNA expression of TNF-α and IL-6 with IC_{50} values of 15.3–52.4 μM.

1. Introduction

The *Schefflera* genus in the Araliaceae family includes about 1100 species worldwide, of which 35 are distributed in the south of China (Wang et al., 2014; Wu et al., 2007). Some species have been used as folk medicines to treat pain, such as that due to rheumatoid arthritis, traumatic injury, fever, and sprains (Hu et al., 1998; Wu et al., 1990). In previous studies of the genus, triterpenes, diterpenes, sesquiterpenes, lignans, and phenolic acids have been identified as bioactive constituents (Nguyen et al., 2015; Wang et al., 2013), some of which reportedly possess anti-inflammatory, antifungal, antiviral, and cytotoxic activities (Cioffi et al., 2003; Li et al., 2007; Muir et al., 1982; Wu et al., 2014). The leaves and twigs of *Schefflera kwangsiensis* are used to prepare Campo Peach Twig Tablets, which are recorded in the Chinese Pharmacopoeia (2010) (Sang et al., 2015) and are currently commercially available as anti-inflammatory and analgesic drugs. Our recent studies of bioactive triterpenoid saponins from *S. kwangsiensis* (Wang et al., 2014, 2016) inspired our further study of another folk medicine from the same genus, *Schefflera rubriflora* C. J. Tseng & G. Hoo, for which the phytochemistry and bioactivity have not been reported.

Inflammatory cytokines are a class of endogenous polypeptides produced by immune system cells to mediate various immune responses. Tumor necrosis factor-α (TNF-α) and interleukine-6 (IL-6) are the most potent mediators of the immune response by macrophages, and both are known to be involved in pain, stiffness, and swelling responses (Lai et al., 2018; Liu et al., 2017; Luo et al., 2018). Previous studies have indicated that exposure to lipopolysaccharide (LPS) can effectively promote the mRNA expression of TNF-α and IL-6 in RAW 264.7 macrophages (Kong et al., 2019; You et al., 2013). Therefore, inhibiting TNF-α and IL-6 activation might be clinically effective in patients with pain and inflammation.

In this study, a 95% ethanol extract of *S. rubriflora* leaves and twigs significantly inhibited ear inflammation in mice caused by croton oil (33.6% inhibition), suggesting potential anti-inflammatory bioactivity. In the further search for anti-inflammatory compounds, the activity-guided isolation of the EtOAc and *n*-BuOH fractions of the 95% ethanol extract was performed, which demonstrated 35.7% and 40.6% inhibitions of croton oil-induced ear inflammation in mice, respectively. Eight undescribed terpenes (**1**–**8**) were obtained, with compounds **2**–**5** exhibiting moderate TNF-α and IL-6 inhibition *in vitro*, consistent with the anti-inflammatory bioactivities of the 95% ethanol extract and its EtOAc and *n*-BuOH fractions *in vivo*.

This paper describes the isolation, structural elucidation, and evaluation of the anti-inflammatory activities of these compounds.

* Corresponding author.
E-mail addresses: lifenghua@imm.ac.cn (F. Li), jianzhang@hotmail.com (J. Zhang), mingbaolin@imm.ac.cn (M. Lin), sxmxiaomuchong@163.com (X. Su), chklee2015@163.com (C. Li), wanghongqing@imm.ac.cn (H. Wang), libaoming@imm.ac.cn (B. Li), rych@imm.ac.cn (R. Chen), jiekang@imm.ac.cn (J. Kang).

https://doi.org/10.1016/j.phytochem.2019.03.021
Received 30 December 2018; Received in revised form 19 March 2019; Accepted 22 March 2019

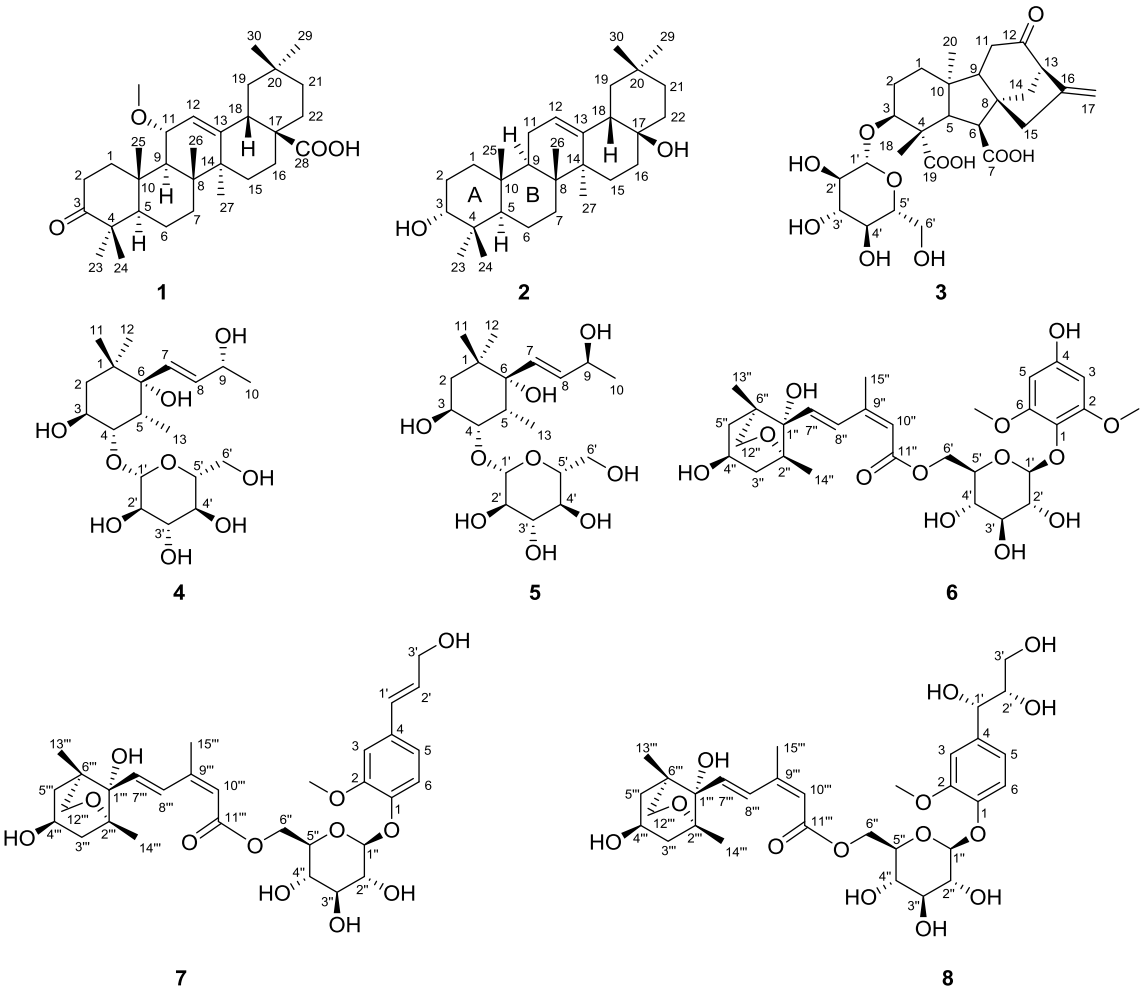

Fig. 1. Structures of compounds **1–8**.

2. Results and discussion

The EtOAc fraction of the 95% EtOH extract of *S. rubriflora* leaves and twigs yielded two undescribed triterpenes (**1** and **2**), whereas the *n*-BuOH fraction yielded five undescribed compounds: one diterpene glycoside (**3**), two megastigmane glycosides (**4** and **5**), and three sesquiterpene esters (**6–8**). The structures of **1–8** (Fig. 1) were elucidated by spectroscopic analysis.

Compound **1** was assigned with the molecular formula $C_{31}H_{48}O_4$ from the high-resolution electrospray ionization mass spectrometry (HRESIMS) peak at *m/z* 483.3479 $[M - H]^-$ (calcd. for $C_{31}H_{47}O_4$, 483.3480) in negative ion mode, which suggested that it had eight degrees of unsaturation. The IR spectrum of **1** suggested the presence of carbonyl (1756, 1705 cm^{-1}) and olefinic (1603 cm^{-1}) groups. The ^1H NMR spectrum (Table 1) showed seven singlet methyl groups [δ_H 1.39, 1.35, 1.18, 1.05 (2), 1.00, and 0.94], one methoxy group [δ_H 3.25 (3H, s, 11-OCH_3)], and one olefinic proton [δ_H 5.78 (1H, br s, H-12)]. In the ^{13}C NMR spectrum (Table 1), two typical olefinic carbon signals at δ_C 122.6 and 148.5, a carboxylic carbon signal at δ_C 181.1, and a carbonyl carbon signal at δ_C 216.8 were observed. According to the NMR and HRESIMS data, the structure of **1** was similar to that of 3-oxoolean-12-en-28-acid (Li et al., 2012), except that **1** contained an extra methoxy group at C-11. The positioning of this methoxy at C-11 was deduced from the heteronuclear multiple bond correlation (HMBC) cross-peaks of 11-OCH_3 (δ_H 3.25)/C-11 (δ_C 76.6). Since H-18 may have an α- or β-orientation in the skeleton of oleanolic acid (Seebacher et al., 2003), NOE experiments were performed. The strong NOEs of H-18 (δ_H 3.38, m)/H_3-30 (δ_H 1.00, s) confirmed the β-orientation of H-18. And the NOEs of H-11 (δ_H 3.87, m)/H_3-25 (δ_H 1.05, s) showed that the 11-OCH_3 group had an α-orientation (Fig. 2). Therefore, compound **1** was identified as 3-oxo-11α-methoxy-olean-12-en-28-oic acid.

According to the HRESIMS spectrum peak at *m/z* 451.3542 $[M + Na]^+$ (calcd. for $C_{29}H_{48}NaO_2$, 451.3546), compound **2** had a molecular formula of $C_{29}H_{48}O_2$ and showed six degrees of unsaturation. The ^1H NMR spectrum (Table 1) contained peaks for seven singlet methyl groups [δ_H 1.23 (2), 1.15, 0.98, 0.95, 0.91, 0.88] and one olefinic proton [δ_H 5.31 (1H, m, H-12)]. The ^{13}C NMR spectrum (Table 1) revealed 29 carbon signals, which indicated that **2** was a nortriterpenoid. The 1D and 2D NMR spectra were consistent with the planar structure of 28-norolean-12-en-3β,17β-diol (Ikuta, 1992). The main difference between these two compounds was the ^{13}C NMR signal at C-3. The C-3 signal for compound **2** appeared at δ_C 75.2 and was 3.0 ppm lower than that of 28-norolean-12-en-3β,17β-diol (δ_C 78.2) (Ikuta, 1992), but the same as that of 3α-hydroxy-11α,12α-epoxyoleanan-28,13β-olide (δ_C 75.1) (Ikuta, 1992). In addition, the NOEs of H-3 (δ_H 3.62, m)/H_3-23 (δ_H 0.91, s) and H-3 (δ_H 3.62, m)/H_3-24 (δ_H 1.23, s) further proved H-3 is in the equatorial orientation (Fig. 3). From the above data, we presumed that **2** contained a 3α-hydroxy group. Therefore, compound **2** was identified as 28-norolean-12-en-3α,17β-diol.

The molecular formula of compound **3** was assigned as $C_{26}H_{36}O_{11}$ by HRESIMS analysis (*m/z* 523.2184 $[M - H]^-$, calcd. for $C_{26}H_{35}O_{11}$, 523.2185). The ^{13}C NMR spectrum showed the presence of a C_{20}-gibberellin diterpene as an aglycone, and was characterized by two tertiary methyl groups at δ_C 29.3 and 15.5, one olefinic carbon at δ_C 145.4, one exocyclic methylene carbon at δ_C 110.5, two carboxyl carbons at δ_C 178.6 and 175.5, and one keto carbonyl group at δ_C 207.8. The NOEs of

Table 1
^{1}H NMR and ^{13}C NMR spectroscopic data of compounds **1** − **5**.

Position	**1**[a]		**2**[a]		position	**3**[b]		**4**[c]		**5**[d]	
	δ_H (*J* in Hz)	δ_C	δ_H (*J* in Hz)	δ_C		δ_H (*J* in Hz)	δ_C	δ_H (*J* in Hz)	δ_C	δ_H (*J* in Hz)	δ_C
1	1.75, m	40.8, CH_2	1.93, m	33.6, CH_2	1	2.41, m	43.7, CH_2		40.2, C		39.3, C
	2.23, m		1.40, m			0.98, m					
2	2.45, m	34.6, CH_2	1.74, m	26.3, CH_2	2	1.95, m	46.3, CH_2	1.99, br d (15.2)	39.5, CH_2	2.06, br d (15.2)	38.6, CH_2
	2.62, m					0.99, m		1.50, br d (15.2)		1.36, br d (15.2)	
3		216.8, C	3.62, m	75.2, CH	3	3.97, m	72.5, CH	4.12, m	69.9, CH	4.05, m	68.4, CH
4		48.2, C		37.9, C	4		43.8, C	3.88, m	84.3, CH	3.85, m	82.9, CH
5	1.37, m	56.0, CH	2.54, m	48.7, CH	5	1.87, d (12.6)	55.9, CH	2.40, m	35.2, CH	2.36, m	33.3, CH
6	1.50, m	20.4, CH_2	1.57, m	18.7, CH_2	6	3.27, d (12.6)	49.8, CH		82.5, C		80.2, C
			1.47 (m)								
			1.47, m		7		175.5, C	5.67, br s	135.0, CH	5.55, d (15.7)	132.9, CH
7	2.03, m	33.4, CH_2	1.40, m	33.5, CH_2	8		48.5, C	5.67, br s	135.6, CH	5.73, dd (15.7,6.0)	135.3, CH
	1.82, m				9	1.45, dd (10.2,7.8)	52.0, CH	4.41, m	71.0, CH	4.29, m	69.4, CH
8		42.9, C		40.2, C	10		44.7, C	1.28, d (6.4)	25.2, CH_3	1.24, d (6.4)	24.3, CH_3
9	1.89, d (8.5)	52.5, CH	2.03, m	48.1, CH	11	2.36, m	35.5, CH_2	1.10, s	29.3, CH_3	1.11, s	27.8, CH_3
10		38.5, C		37.6, C		2.11, m					
11	3.87, m	76.6, CH	1.26, m	24.0, CH_2	12		207.8, C	0.88, s	27.9, CH_3	0.85, s	26.6, CH_3
12	5.78, br s	122.6, CH	5.31, m	122.7, CH	13	3.06, br s	56.4, CH	1.01, d (7.2)	14.6, CH_3	1.04, d (7.2)	13.1, CH_3
13		148.5, C		145.7, C	14	2.00, d (12.0)	36.7, CH_2				
14		43.3, C		42.1, C		1.84, dd (12.0,4.8)					
15	2.08, m	28.8, CH_2	2.54, m	26.4, CH_2	15	2.20, d (15.6)	45.9, CH_2				
16	2.08, m	24.0, CH_2	2.14, m	28.1, CH_2		2.13, d (15.6)					
	1.96, m		1.00, m		16		145.4, C				
17		46.9, C		71.0, C	17	4.99, s	110.5, CH_2				
18	3.38, m	42.2, CH	1.74, m	49.4, CH	18	1.14, s	29.3, CH_3				
19	1.79, m	46.6, CH_2	1.73, m	48.9, CH_2	19		178.6, C				
	1.35, m				20	0.76, s	15.5, CH_3				
20		31.4, C		31.2, C	1′	4.18, d (7.8)	102.2, CH	4.44, d (8.0)	103.9, CH	4.27, d (7.8)	102.9, CH
21	1.42, m	35.2, CH_2	1.37, m	37.1, CH_2	2′	2.87, t (8.4)	73.6, CH	3.29, t (8.0)	75.6, CH	3.28, t (7.8)	75.1, CH
	1.21, m		1.27, m		3′	3.12, t (8.4)	76.8, CH	3.49, t (8.0)	78.8, CH	3.33, t (7.8)	78.2, CH
22	1.36, m	33.5, CH_2	1.99, m	38.8, CH_2	4′	3.01, m	70.1, CH	3.40, t (8.0)	72.6, CH	3.13, t (7.8)	71.8, CH
	1.20, m				5′	3.05, m	76.7, CH	3.35, m	78.5, CH	3.24, m	78.3, CH
23	1.18, s	27.0, CH_3	0.91, s	29.4, CH_3	6′	3.63, d (11.4)	61.1, CH_2	3.92, d (12.0)	63.5, CH_2	3.86, d (12.0)	63.0, CH_2
24	1.05, s	22.0, CH_3	1.23, s	22.8, CH_3		3.40, dd (11.4,4.8)		3.72, dd (12.0,5.2)		3.67, dd (12.0,6.0)	
25	1.05, s	16.9, CH_3	0.98, s	15.4, CH_3							
26	1.39, s	19.3, CH_3	1.23, s	18.0, CH_3							
27	1.35, s	25.8, CH_3	1.15, s	25.7, CH_3							
28		181.1,C									
29	0.94, s	33.6, CH_3	0.88, s	33.0, CH_3							
30	1.00, s	24.1, CH_3	0.95, s	24.1, CH_3							
11-OCH_3	3.25, s	54.6, OCH_3									

[a] Recorded in pyridine-d_5.
[b] Recorded in DMSO-d_6.
[c] Recorded in D_2O.
[d] Recorded in CD_3OD.

H-3 (δ_H 3.97, m)/H_3-20 (δ_H 0.76, s) and H_3-20 (δ_H 0.76, s)/H-6 (δ_H 3.27, d, J = 12.6 Hz) confirmed that H-3 was α-oriented (Fig. 2). Therefore, the structure of the aglycone of **3** was consistent with that of 12-oxo-GA_{14} (Gaskin et al., 1984). The HMBC correlations of H-1′ (δ_H 4.18, d, J = 7.8 Hz)/C-3 (δ_C 72.5) indicated that a glucosyl residue was connected to the hydroxy group at C-3 (Fig. 2). The absolute configuration of the sugar unit was identified as D-glucose by HPLC analysis after acid hydrolysis and derivatization (Su et al., 2018). Compound **3** was identified as 12-oxo-GA_{14}-3-*O*-β-D-glucopyranoside.

Compound **4** was assigned the molecular formula $C_{19}H_{34}O_9$ from its HRESIMS results (*m/z* 429.2087 $[M + Na]^+$, calcd. for $C_{19}H_{34}NaO_9$, 429.2095) and had three degrees of unsaturation. The IR spectrum of **4** showed absorption bands at 3368, 1452, and 1079 cm^{-1}, which indicated the presence of hydroxy, olefinic, and ether groups, respectively. The peaks in the ^{1}H NMR, ^{13}C NMR, HSQC, and HMBC spectra of **4**, except for the six signals of the glucosyl unit, were consistent with the planar structure of wilsonol B (Shu et al., 2013). According to the HMBC correlations of H-1′ (δ_H 4.44, d, J = 8.0 Hz)/C-4 (δ_C 84.3), the sugar moiety was attached to the 4-position of the aglycone (Fig. 2). To further unambiguously confirm the relative and absolute configurations of **4**, its aglycone (**4a**) was obtained using enzymatic hydrolysis (Gu et al., 2013). The relative configuration of **4a** was determined from the coupling constants (see 4.5.1) and NOE data (Fig. 3). The NOEs of H-5 (δ_H 2.23)/H-7 (δ_H 5.55) and H-5 (δ_H 2.23)/H_3-11 (δ_H 1.14) determined the axial-axial relationships between H-5 and H-11, and between H-5 and H-7, the latter of which confirmed the substituting group containing H-7 is equatorially oriented (Fig. 3). It also clarified the same orientations (β) of H-5, H-7, and H-11. In addition, the $J_{H\text{-}5\text{-}H\text{-}4}$ (2.8 Hz) and $J_{H\text{-}4\text{-}H\text{-}3}$ (3.2 Hz) values confirmed axial-equatorial and equatorial-equatorial couplings, respectively. The absolute configuration of C-9 in the side chain of **4a** was determined to be *R* using Mosher's method (Fig. S98) (Shu et al., 2013). The absolute configuration of the cyclohexane ring in **4a** was established by comparing experimental and calculated electronic circular dichroism (ECD) data (Fig. 4), which gave only two possible candidate stereoisomers, **4a-1** and **4a-2** (Fig. 4). Conformational analysis of **4a-1** showed nine lowest-energy conformers. These conformers were further optimized at the B3LYP/6-31G(d) level. The ECD spectra of the different conformers were simulated with a half-bandwidth of 0.35 eV, and the overall theoretical ECD spectra were obtained according to the Boltzmann weighting of each conformer. The experimental ECD spectrum of **4a** [λ_{max} ($\Delta\varepsilon$) 200 (−3.63)] was similar to the calculated ECD curve of **4a-1** (3*S*, 4*S*, 5*R*, 6*R*), but the opposite of that of **4a-2** (3*R*, 4*R*, 5*S*, 6*S*) (Fig. 4). Therefore, the relative and absolute configurations of **4a** were totally consistent

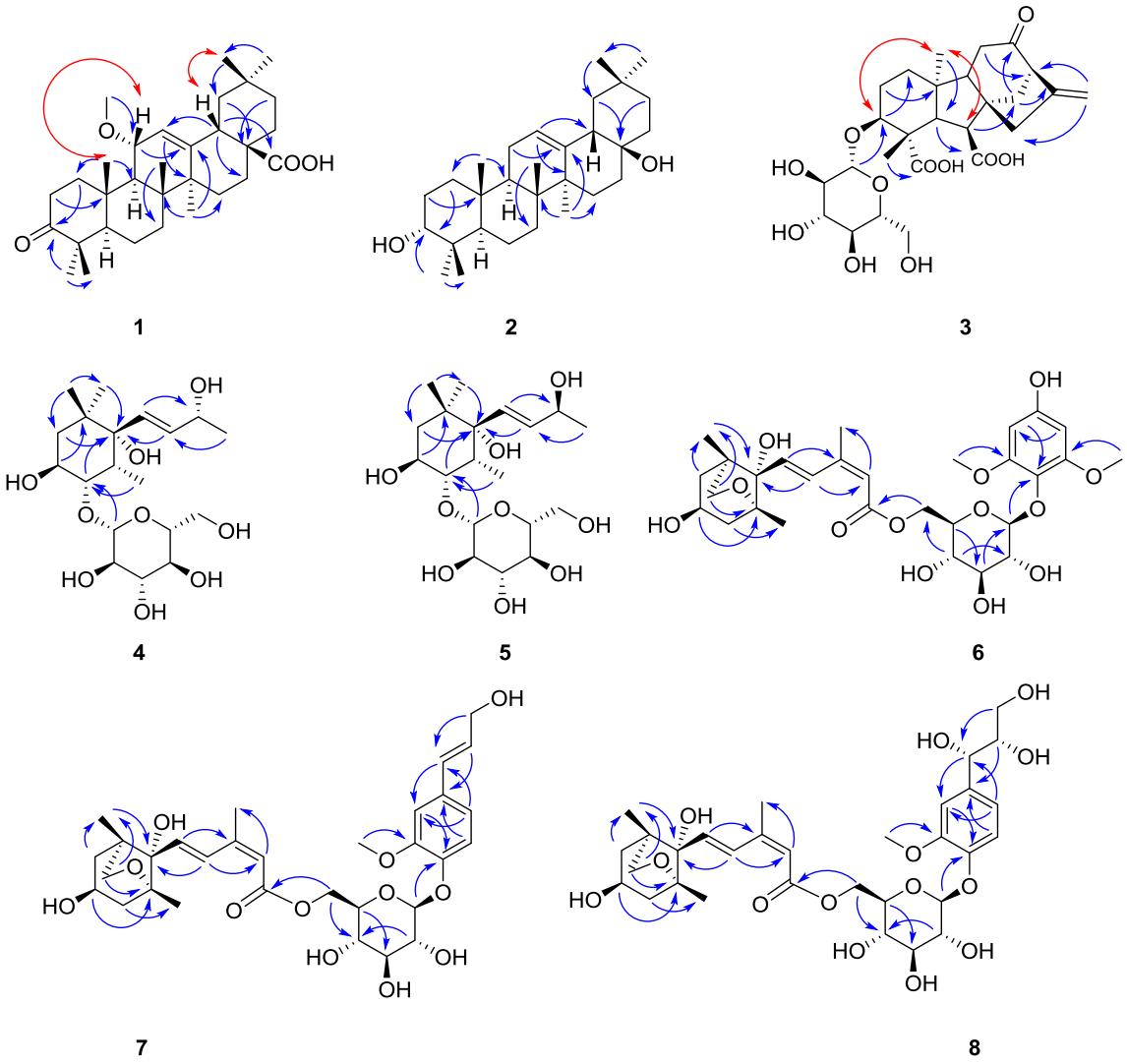

Fig. 2. Key HMBC correlations (blue arrow) and NOEs (red arrow) of compounds **1**–**8**. (For interpretation of the references to colour in this figure legend, the reader is referred to the Web version of this article.)

with those of wilsonol B (Shu et al., 2013). The absolute configuration of the sugar unit was assigned as D-glucose by HPLC analysis of thiocarbamoyl-thiazolidine derivatives of the acid hydrolysis product (Su et al., 2018). Therefore, compound **4** was named as (3*S*,4*S*,5*R*,6*R*,7*E*,9*R*)-3,6,9-trihydroxy-megastigm-7-en-4-*O*-*β*-D-glucopyranoside.

Compound **5** gave the same HRESIMS ion at *m/z* 429.2092 [M + Na]$^+$ (calcd. for $C_{19}H_{34}NaO_9$, 429.2095) as compound **4**, which meant it had the same molecular formula ($C_{19}H_{34}O_9$). The ^{1}H NMR, ^{13}C NMR, HSQC, and HMBC spectra showed that compounds **4** and **5** had the same planar structure. The stereostructure of **5** was determined after hydrolysis. The hydrolysate of **5** (**5a**) (Figs. 3 and 5) had the same relative and absolute configurations as **4a** (Figs. 3 and 4), except for the configuration of C-9, which was confirmed to be *S* using Mosher's method (Fig. S98) (Shu et al., 2013). Therefore, the aglycone of **5** was unambiguously identified as wilsonol A (Shu et al., 2013). The absolute configuration of the sugar residue was determined to be D-glucose by HPLC analysis after acid hydrolysis and derivatization (Su et al., 2018). Therefore, compound **5** was named as (3*S*,4*S*,5*R*,6*R*,7*E*,9*S*)-3,6,9-trihydroxy-megastigm-7-en-4-*O*-*β*-D-glucopyranoside.

According to the HRESIMS signal at *m/z* 595.2383 [M – H]$^-$ (calcd. for $C_{29}H_{39}O_{13}$, 595.2396) in negative ion mode, the molecular formula of **6** was $C_{29}H_{40}O_{13}$. The IR spectrum contained absorption bands for hydroxy (3363 cm^{-1}), carbonyl (1706 cm^{-1}), phenyl (1600, 1508 cm^{-1}), olefinic (1452 cm^{-1}), and ether (1048 cm^{-1}) groups. The ^{1}H and ^{13}C NMR spectra showed **6** contained sesquiterpene, phenyl, and glycosyl moieties. The sesquiterpene moiety was determined to be a dihydrophaseic group, featuring three methyl groups {CH_3-15″ [δ_H 2.12

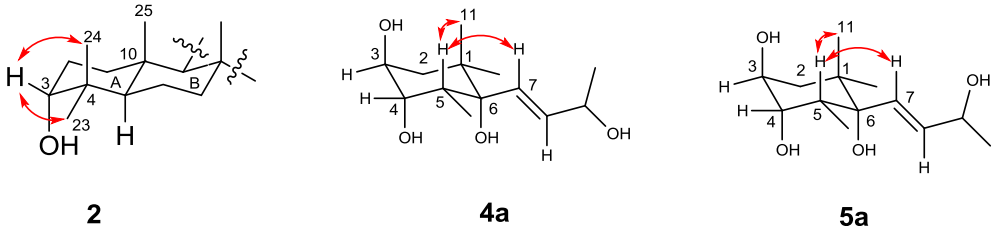

Fig. 3. Key NOEs of **2**, **4a** and **5a**.

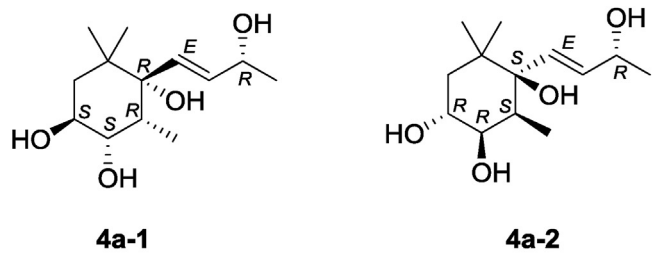

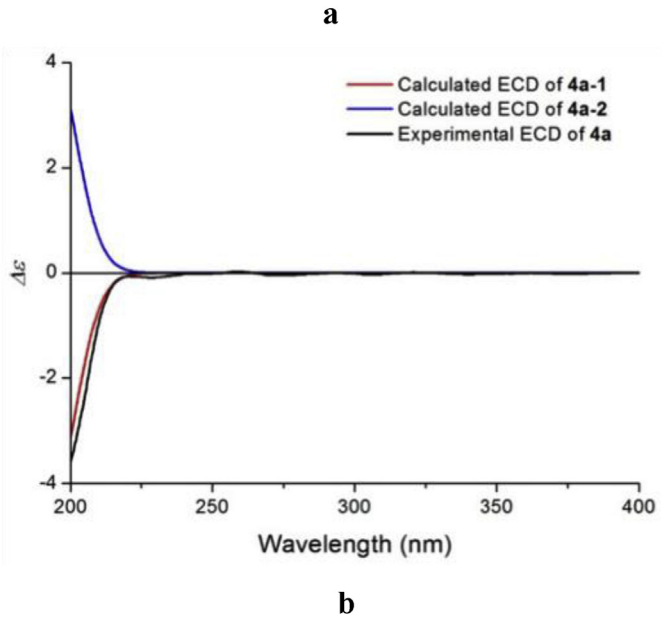

Fig. 4. (a) Structures of **4a-1** and **4a-2**; (b) experimental ECD spectrum of **4a** in MeOH and calculated ECD spectra of **4a-1** and **4a-2**.

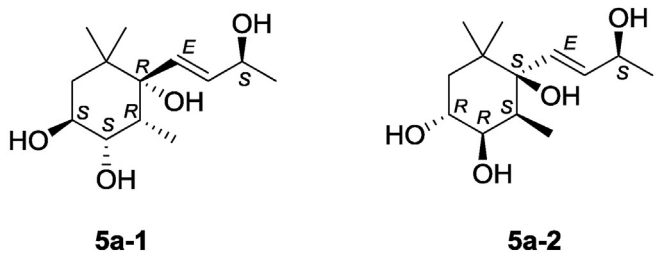

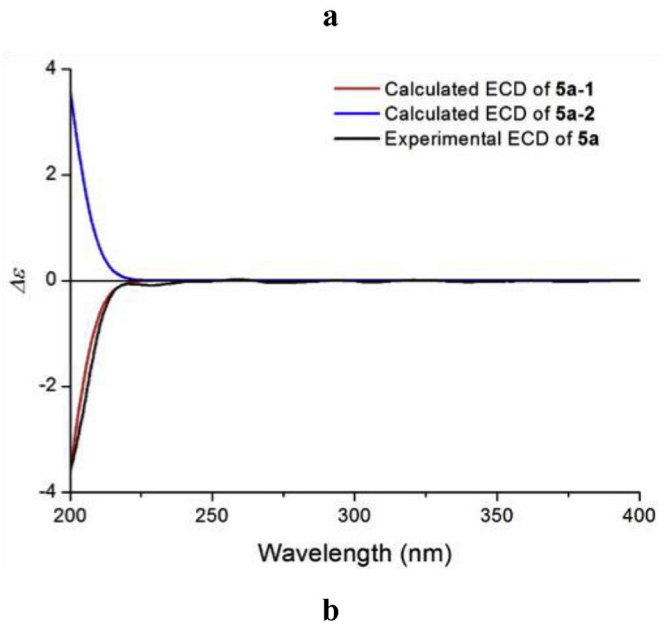

Fig. 5. (a) Structures of **5a-1** and **5a-2**; (b) experimental ECD spectrum of **5a** in MeOH and calculated ECD spectra of **5a-1** and **5a-2**.

(3H, s), δ_C 21.3], CH_3-14″ [δ_H 1.18 (3H, s), δ_C 19.7], and CH_3-13″ [δ_H 0.95 (3H, s), δ_C 16.4]}, three methylenes {CH_2-12″ [δ_H 3.84 (d, J = 7.2 Hz), 3.74 (d, J = 7.2 Hz); δ_C 77.3], CH_2-3″ [δ_H 2.08 (dd, J = 13.6, 6.4 Hz), 1.78 (dd, J = 13.6, 10.4 Hz); δ_C 46.0], and CH_2-5″ [δ_H 1.89 (dd, J = 13.6, 7.2 Hz), 1.68 (m); δ_C 44.6]}, two coupled olefinic methines {CH-8″ [δ_H 8.00 (d, J = 15.6 Hz); δ_C 131.7] and CH-7″ [δ_H 6.58 (d, J = 15.6 Hz); δ_C 135.8]}, one olefinic methine {CH-10″ [δ_H 5.76 (s); δ_C 118.5]}, one oxygenated methine {CH-4″ [δ_H 4.13 (m), δ_C 66.0]}, one carbonyl group C-11″ (δ_C 167.3), and four quaternary carbons {[δ_C 152.1 (C-9″), 87.8 (C-2″), 83.3 (C-1″), and 49.6 (C-6″)]}. The $C_{7''}$ = $C_{8''}$ double bond had a *trans* configuration. Other signals were attributed to a 2,6-dimethoxy-*p*-hydroquinone-1-*O*-glucopyranosyl moiety. The HMBC correlations between H-6′ (δ_H 4.39) and C-11″ (δ_C 167.3) showed that these two moieties were linked (Fig. 2). Compound **6** was hydrolyzed under alkaline conditions to obtain dihydrophaseic acid (**6a**) (Milborrow, 1975; Zhang et al., 2010) and 2,6-dimethoxy-*p*-hydroquinone-1-*O*-*β*-glucopyranoside (**6b**) (Otsuka et al., 1989) (Fig. 6). The relative configuration of **6a** was assigned according to the NOE spectrum. The NOEs of H-4″ (δ_H 4.08, m)/H-12″ (δ_H 3.77, d, J = 7.2 Hz), H_3-13″ (δ_H 0.89, s)/H-7″ (δ_H 6.48, d, J = 16.2 Hz), and H_3-14″ (δ_H 1.11, s)/H-7″ (δ_H 6.48, d, J = 16.2 Hz) indicated that H-4″ and CH_2-12″ had *α*-orientations, whereas H_3-13″, H_3-14″, and CH-7″ had *β*-orientations (Fig. 6). The NOEs of H_3-15″ (δ_H 2.04, s)/H-7″ (δ_H 6.48, d, J = 16.2 Hz) and H-10″ (δ_H 5.73, s) reflected the *Z* geometry of the terminal double bond ($C_{9''}$ = $C_{10''}$) in **6a** (Fig. 6). ECD calculations were used to determine the absolute configuration of compound **6a**. The experimental ECD spectrum of dihydrophaseic acid (**6a**) showed a negative Cotton effect at 259 nm ($\Delta\varepsilon$ = – 0.949) (Fig. 7). Two stereoisomers, **6a-1** and **6a-2**, were considered as candidates for the ECD calculations. The seven lowest-energy conformers of **6a-1** were obtained after conformational analysis. The conformers were further optimized at the APFD/6-31g(d)level. Theoretical ECD spectra were then obtained according to the Boltzmann weighting of each conformer. Comparison of the calculated ECD spectrum of **6a-1** with the experimental ECD spectrum of **6a** showed good agreement. Therefore, the absolute configuration of **6a** was determined to be 1″*S*,2″*R*,4″*S*,6″*R*. The absolute configuration of the glucosyl residue was established as D-glucose by HPLC analysis after acid hydrolysis and derivatization of **6b** (Su et al., 2018). Therefore, compound **6** was assigned as 2,6-dimethoxy-*p*-hydroquinone-1-*O*-*β*-D-[6′-*O*-(1″*S*,2″*R*,4″*S*,6″*R*,7″*E*,9″*Z*)-dihydrophaseyl]-glucopyranoside.

The positive-ion HRESIMS of **7** contained a peak for a sodiated molecular ion at *m/z* 629.2558 (calcd. for $C_{31}H_{42}NaO_{12}$, 629.2568), which corresponded to a molecular formula of $C_{31}H_{42}O_{12}$. The ^{1}H NMR spectrum showed that **7** also contained a dihydrophaseic moiety (**7a**) that was the same as that of **6a**. The other signals included one ABX system (δ_H 7.06, d, J = 1.6 Hz; 7.02, d, J = 8.0 Hz; 6.88, dd, J = 8.0, 1.6 Hz), two olefinic signals (δ_H 6.53, d, J = 16.0 Hz; 6.28, dt, J = 16.0, 5.6 Hz), one oxygenated methylene (δ_H 4.22, 2H, dd, J = 5.6, 1.2 Hz), and six glucosyl signals [δ_H 4.85 (overlapped), 4.40 (2H, m), 3.65 (m), 3.52 (t, J = 7.8 Hz), 3.47 (t, J = 8.4 Hz), and 3.41 (t, J = 8.4 Hz)], which were assigned to a 4-(3′-hydroxypropenyl)-2-methoxyphenyl-1-*O*-glycopyranosyl moiety (Zhou et al., 2000). The HMBC correlations of H-6″ (δ_H 4.40, m)/C-11‴ (δ_C 167.4) confirmed that these two moieties were connected (Fig. 2). The absolute configuration of the glucosyl residue was established as D-glucose by HPLC analysis after acid hydrolysis and derivatization of **7b** (Su et al., 2018), which was obtained after basic hydrolysis of **7** (Hong et al., 2017). Compound **7** was

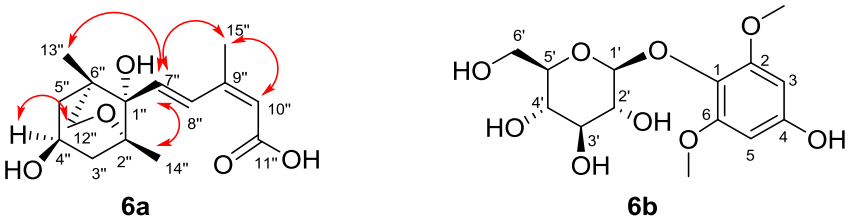

Fig. 6. Structure and key NOEs of **6a**; Structure of **6b**.

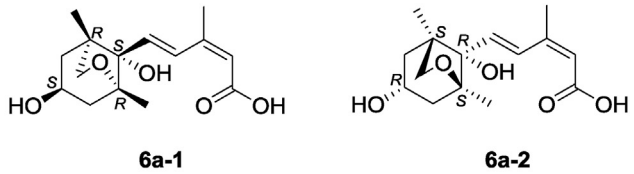

a

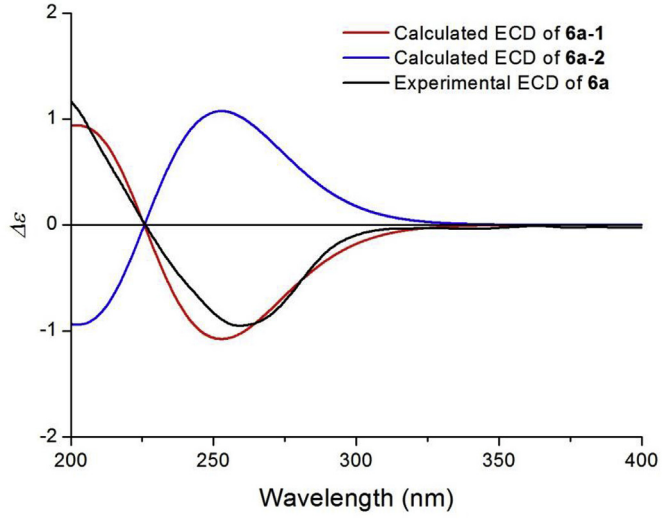

b

Fig. 7. (a) Structures of **6a-1** and **6a-2**; (b) experimental ECD spectrum of **6a** in MeOH and calculated ECD spectra of **6a-1** and **6a-2**.

assigned as 4-(3′-hydroxypropenyl)-2-methoxyphenyl-1-*O*-*β*-D-{6″-*O*-[(1‴*S*,2‴*R*,4‴*S*,6‴*R*,7‴*E*,9‴*Z*)-dihydrophaseic acyl]}-glucopyranoside.

Compound **8** had a molecular formula of $C_{31}H_{44}O_{14}$, which was deduced from the HRESIMS ion at *m/z* 663.2634 (calcd. for $C_{31}H_{44}NaO_{14}$, 663.2623). The ^{1}H and ^{13}C NMR spectra of **8** (Table 2) were similar to those of **7**. However, two olefinic resonances in the spectrum of **7** were replaced by two oxygenated methine signals [H-1′ (δ_H 4.61, d, J = 5.6 Hz), C-1′ (δ_C 76.4); and H-2′ (δ_H 3.82, m), C-2′ (δ_C 78.3)] in the spectrum of **8**. To confirm the relative configuration of the two additional hydroxy groups, basic hydrolysis was performed to obtain **8a** and **8b** (Hong et al., 2017). The structure of **8a** is the same as those of **6a** and **7a**. The structure of **8b** was determined to be 2-methoxy-4-(1′,2′,3′-trihydroxypropyl)-phenyl-1-*O*-glucopyranoside by comparison of its HRESIMS, ^{1}H NMR, and ^{13}C NMR data with those reported in the literature (Comet et al., 1997; Ishikawa et al., 2002). The ^{13}C NMR chemical shifts of the two oxygenated methines (C-1′: δ_C 74.5; and C-2′: δ_C 77.6) in **8b** were similar to the corresponding ^{13}C NMR signals in *threo*-2-methoxy-4-(1′,2′,3′-trihydroxypropyl)-phenol (C-1′: δ_C 74.9; C-2′: δ_C 77.8) (Ishikawa et al., 2002), but different from those in *erythro*-2-methoxy-4-(1′,2′,3′-trihydroxypropyl)-phenol (C-1′: δ_C 76.1; C-2′: δ_C 76.5) (Ishikawa et al., 2002), which suggested that H-1′ and H-2′ of **8b** were in the *threo* form. Compound **8b** was further hydrolyzed using snailase to obtain the aglycone (**8b-1**) (Gu et al., 2013). The absolute configurations of H-1′ and H-2′ were confirmed according to the reported optical values. A negative optical value would indicate the 1′*R*,2′*R* form of *threo*-2-methoxy-4-(1′,2′,3′-trihydroxypropyl)-phenol and a positive optical value would indicate the 1′*S*,2′*S* form of *threo*-2-methoxy-4-(1′,2′,3′-trihydroxypropyl)-phenol (Takeshita et al., 1992; Ishikawa et al., 2002). Therefore, **8b-1** was confirmed to be 2-methoxy-4-[(1′*S*,2′*S*)-1′,2′,3′-trihydroxypropyl]-phenol due to its positive optical value. The absolute configuration of the glucosyl residue was established as D-glucose by HPLC analysis after acid hydrolysis and derivatization of **8b** (Su et al., 2018). Therefore, **8** was assigned as 2-methoxy-4-[(1′*S*,2′*S*)-1′,2′,3′-trihydroxypropyl]-phenyl-1-*O*-*β*-D-{6″-*O*-[(1‴*S*,2‴*R*,4‴*S*,6‴*R*,7‴*E*,9‴*Z*)-dihydrophaseic acyl]}-glucopyranoside.

The 95% ethanol extract and its EtOAc and *n*-BuOH fractions of *S. rubriflora* leaves and twigs significantly inhibited ear inflammation in mice caused by croton oil, with 33.6%, 35.7%, and 40.6% inhibition ($P < 0.05$) compared to the control group.

To identify the anti-inflammatory components of the 95% ethanol extract of *S. rubriflora*, the isolated compounds were tested for TNF-*α* and IL-6 inhibition. Compounds **2–5** inhibited mRNA expression of TNF-*α* and IL-6 in LPS-induced RAW 264.7 macrophages, with IC_{50} 15.3–52.4 *μ*M (Table 3).

3. Conclusion

The present study demonstrated the anti-inflammatory effects of a 95% EtOH extract of *S. rubriflora in vivo*. Eight previously undescribed triterpenes and triterpene glycosides (compounds **1–8**) were isolated from the 95% EtOH extract of *S. heptaphylla*, four of which (**2–5**) showed anti-inflammatory activity, with the inhibition of TNF-*α* and IL-6 in LPS-induced RAW 264.7 macrophages (IC_{50} 15.3–52.4 *μ*M). The only structural difference between **4** and **5** is the absolute configuration at C-9, which may have caused the different anti-inflammatory activity: the TNF-*α* and IL-6 inhibition of 9*R* (**4**) are both better than that of 9*S* (**5**). Three ester derivatives (**6–8**) consisting of sesquiterpenes and phenolic glycosyl moieties were newly determined, and shown not to be artefacts using HPLC/(+)ESIMS (Fig. S97).

4. Experimental

4.1. General experimental procedures

Optical rotation was measured using a Jasco P-2000 digital polarimeter (Jasco, Tokyo, Japan). UV spectra were collected in methanol using a Jasco V-650 UV–Vis spectrophotometer. Fourier-transform infrared spectroscopy was performed using a Nicolet 5700 ATR-FTIR spectrometer (Thermo Fisher Scientific, Waltham, MA, USA). ^{1}H and ^{13}C NMR spectra were acquired using a Bruker Avance III 400 MHz (or 500 MHz) NMR spectrometer (Bruker BioSpin GmbH, Rheinstetten, Germany) or an Agilent VNMRS 600 MHz NMR spectrometer (Palo Alto, CA, USA). HRESIMS spectra were recorded with an Agilent 1200 SL series LC/6520 QTOF spectrometer (Agilent, Boblingen, Germany) or a Thermo Fisher Scientific Q Exactive Focus Hybrid Quadrupole-Orbitrap mass spectrometer (Waltham, MA, USA). Sephadex LH-20 (GE Healthcare Bio-Sciences AB, Uppsala, Sweden) and C-18 (50 *μ*m; YMC,

Table 2
^{1}H NMR and ^{13}C NMR spectroscopic data of compounds **6** − **8**.

Position	**6**[a]		position	**7**[a]		**8**[b]	
	δ_H (*J* in Hz)	δ_C		δ_H (*J* in Hz)	δ_C	δ_H (*J* in Hz)	δ_C
1		129.3, C	1		147.4, C		147.8, C
2		154.9, C	2		150.2, C		151.4, C
3	6.13, s	94.0, CH	3	7.06, d (1.6)	111.4, CH	7.05, s	113.7, CH
4		156.1, C	4		133.7, C		138.9, C
5	6.13, s	94.0, CH	5	6.88, dd (8.0, 1.6)	120.6, CH	6.85, d (8.0)	122.1, CH
6		154.9, C	6	7.02, d (8.0)	118.2, CH	7.01, d (8.0)	118.8, CH
1′	4.64, d (7.8)	106.1, CH	1′	6.53, d (16.0)	131.3, CH	4.61, d (5.6)	76.4, CH
2′	3.44, m	75.5, CH	2′	6.28, dt (16.0, 5.6)	128.9, CH	3.82, m	78.3, CH
3′	3.45, m	77.8, CH	3′	4.22, dd, (5.6, 1.2)	63.7, CH_2	3.49, dd (12.0, 3.0)	65.3, CH_2
4′	3.43, m	71.7, CH				3.39, dd (12.0, 6.6)	
5′	3.53, m	75.6, CH	1″	4.85, overlapped	102.7, CH	5.00, d (6.4)	103.4, CH
6′	4.39, d, (12.0)	64.1, CH_2	2″	3.52, t, (7.8)	74.9, CH	3.63, m	75.6, CH
	4.33, dd (12.0,3.6)		3″	3.47, t, (8.4)	77.8, CH	3.85, m	78.3, CH
1″		83.3, C	4″	3.41, t, (8.4)	71.8, CH	3.57, t (9.0)	72.8, CH
2″		87.8, C	5″	3.65, m	75.6, CH	3.67, m	76.3, CH
3″*α*	2.08, dd (13.6, 6.4)	46.0, CH_2	6″	4.40, m	64.1, CH_2	4.46, m	65.4, CH_2
3″*β*	1.78, dd (13.6, 10.4)		1‴		83.3, C		85.3, C
4″	4.13, m	66.0, CH	2‴		87.8, C		89.7, C
5″*α*	1.89, dd (13.6, 7.2)	44.6, CH_2	3‴*α*	2.02, m	46.1, CH_2	1.79, m	46.3, CH_2
5″*β*	1.68, m		3‴*β*	1.73, m		1.89, m	
6″		49.6, C	4‴	4.10, m	66.0, CH	4.14, m	67.5, CH
7″	6.58, d (15.6)	135.8, CH	5‴*α*	1.85, m	44.6, CH_2	1.90, m	44.8, CH_2
8″	8.00, d (15.6)	131.7, CH	5‴*β*	1.66, m		1.60, m	
9″		152.1, C	6‴		49.6, C		50.6, C
10″	5.76, s	118.5, CH	7‴	6.56, d (16.0)	135.8, CH	6.51, d (16.2)	136.8, CH
11″		167.3, C	8‴	8.00, d (16.0)	131.7, CH	7.76, d (16.2)	133.2, CH
12″	3.84, d (7.2)	77.3, CH_2	9‴		152.3, C		155.0, C
	3.74, d (7.2)		10‴	5.82, s	118.4, CH	5.85, s	119.6, CH
13″	0.95, s	16.4, CH_3	11‴		167.4, C		170.3, C
14″	1.18, s	19.7, CH_3	12‴	3.88, d (7.2)	77.3, CH_2	3.81, d (7.2)	78.3, CH_2
15″	2.12, s	21.3, CH_3		3.72, d (7.2)		3.73, d (7.2)	
2-OCH_3	3.78, s	56.7, OCH_3	13‴	0.92, s	16.4, CH_3	0.88, s	17.9, CH_3
6-OCH_3	3.78, s	56.7, OCH_3	14‴	1.09, s	19.7, CH_3	1.06, s	21.0, CH_3
			15‴	2.12, s	21.4, CH_3	2.10, s	23.2, CH_3
			2-OCH_3	3.88, s	56.7, OCH_3	3.86, s	58.6, OCH_3

[a] Recorded in CD_3OD.
[b] Recorded in D_2O.

Table 3
The inhibitory effects of compounds **2–5** against LPS-induced mRNA expression of TNF-*α* and IL-6 in RAW 264.7 macrophages.

Compounds	**IC_{50} (*μ*M)**	
	TNF-*α*	**IL-6**
2	52.4 ± 0.10	32.4 ± 0.03
3	44.2 ± 0.02	29.8 ± 0.04
4	24.9 ± 0.01	30.1 ± 0.05
5	39.8 ± 0.03	42.3 ± 0.08
Positive control (kaempferol)	15.3 ± 0.01	18.8 ± 0.03

Kyoto, Japan) columns were used to fractionate the samples. Column chromatography fractions were analyzed by HPLC (Agilent, Boblingen, Germany).

4.2. Plant material

Leaves and twigs of *Schefflera* rubriflora C. J. Tseng & G. Hoo (Araliaceae) were collected in Xishuangbanna District (GPS coordinates: N 21°56′-22°17′, E 100°51′-101°04′), Yunnan Province, China, in June 2013 (summer, wet season) and were identified by Professor Lin Ma of the Institute of Materia Medica, Chinese Academy of Medical Science and Peking Union Medical College, China. A voucher specimen (ID-S-2478) was deposited in the Institute of Materia Medica, Chinese Academy of Medical Science and Peking Union Medical College, China.

4.3. Extraction and isolation

Air-dried, powdered leaves and twigs from *S. rubriflora* (20.1 kg) were extracted with 95% EtOH (3 × 50 L) under reflux conditions for 1.5 h. The combined extracts were concentrated under reduced pressure to afford the crude extract (1.5 kg), which was then suspended in H_2O and successively partitioned with petroleum ether, EtOAc, and *n*-BuOH.

The EtOAc extract (109 g) was subjected to chromatography over silica gel (160–200 mesh) with a gradient elution of petroleum ether–acetone (10:0 → 3:7) to give 12 fractions (1–12). Fraction 2 (23 g) was subjected to chromatography on a C-18 column with a gradient elution of MeOH−H_2O (6:4 → 10:0), followed by a Sephadex LH-20 column (MeOH−H_2O, 8:2), and then further purified by semi-preparative HPLC to afford compounds **1** (25 mg; eluent: CH_3CN−H_2O, 7:3) and **2** (30 mg; CH_3CN−H_2O, 8:2).

The *n*-BuOH fraction (510 g) was subjected to chromatography on a Diaion HP-20 macroporous resin column, and eluted with H_2O followed by 10%, 30%, 50%, 70%, and 95% aq. EtOH. The 30% EtOH fraction (80 g) was subjected to chromatography on a C-18 column, eluting with a gradient of MeOH−H_2O (5:95 → 100:0) to yield 14 fractions (1–14). Fraction 2 (3.4 g) was subjected to chromatography on a Sephadex LH-20 column and further purified by preparative HPLC to yield compounds **3** (36 mg; eluent: MeOH−H_2O, 3:7), **4** (100 mg; MeOH−H_2O, 2:8), and **5** (40 mg; MeOH−H_2O, 2:8). Fraction 6 (4.0 g) was subjected to chromatography on a Sephadex LH-20 column (MeOH−H_2O, 3:7) and then purified by semi-preparative HPLC by isocratic elution with MeOH−H_2O (3:7) to obtain compounds **6** (70 mg), **7** (60 mg), and **8** (88 mg).

4.3.1. 3-Oxo-11α-methoxy-olean-12-en-28-oic acid (1)

White powder; $[\alpha]_D^{20}$ + 10.9 (*c* 0.1, MeOH); UV (MeOH) λ_{max} (log ε) 205 (1.16), 250 (0.71), 255 (0.73) nm; IR ν_{max} 2935, 1756, 1705, 1603 cm^{-1}. For ^1H (500 MHz) and ^{13}C NMR (100 MHz) spectroscopic data, see Table 1. HRESIMS (negative ion) *m/z* 483.3479 $[M - H]^-$ (calcd. for $C_{31}H_{47}O_4$, 483.3480).

4.3.2. 28-Norolean-12-en-3α,17β-diol (2)

White powder; $[\alpha]_D^{20}$ + 51.9 (*c* 0.1, MeOH); UV (MeOH) λ_{max} (log ε) 204 (0.86) nm; IR ν_{max} 3360, 2920, 1631, 1385, 1121, 1071 cm^{-1}. For ^1H (500 MHz) and ^{13}C NMR (125 MHz) spectroscopic data, see Table 1. HRESIMS (positive ion) *m/z* 451.3542 $[M + Na]^+$ (calcd. for $C_{29}H_{48}NaO_2$, 451.3546).

4.3.3. 12-Oxo-GA$_{14}$-3-O-β-D-glucopyranoside (3)

White powder; $[\alpha]_D^{20}$ − 50.4 (*c* 0.1, MeOH); UV (MeOH) λ_{max} (log ε) 206 (0.94), 255 (0.17) nm; IR ν_{max} 3392, 2945, 1701, 1562, 1104, 1080 cm^{-1}. For ^1H (600 MHz) and ^{13}C NMR (150 MHz) spectroscopic data, see Table 1. HRESIMS (negative ion) *m/z* 523.2184 $[M - H]^-$ (calcd. for $C_{26}H_{35}O_{11}$, 523.2185).

4.3.4. (3S,4S,5R,6R,7E,9R)-3,6,9-trihydroxy-megastigm-7-en-4-O-β-D-Glucopyranoside (4)

White powder; $[\alpha]_D^{20}$ − 47.9 (*c* 0.1, MeOH); UV (MeOH) λ_{max} (log ε) 203 (0.65) nm; IR ν_{max} 3368, 2925, 1452, 1079 cm^{-1}. For ^1H (400 MHz) and ^{13}C NMR (100 MHz) spectroscopic data, see Table 1. HRESIMS (positive ion) *m/z* 429.2087 $[M + Na]^+$ (calcd. for $C_{19}H_{34}NaO_9$, 429.2095).

4.3.5. (3S,4S,5R,6R,7E,9S)-3,6,9-trihydroxy-megastigm-7-en-4-O-β-D-Glucopyranoside (5)

White powder; $[\alpha]_D^{20}$ − 43.8 (*c* 0.1, MeOH); UV (MeOH) λ_{max} (log ε) 203 (0.55) nm; IR ν_{max} 3379, 2925, 1452, 1078 cm^{-1}. For ^1H (400 MHz) and ^{13}C NMR (100 MHz) spectroscopic data, see Table 1. HRESIMS (positive ion) *m/z* 429.2092 $[M + Na]^+$ (calcd. for $C_{19}H_{34}NaO_9$, 429.2095).

2,6-Dimethoxy-p-hydroquinone-1-O-β-D-[6′-O-(1″S,2″R,4″S,6″R,7″E,9″Z)-dihydrophaseyl]-glucopyranoside (6)

White powder; $[\alpha]_D^{20}$ − 42.0 (*c* 0.1, MeOH); UV (MeOH) λ_{max} (log ε) 204 (1.82), 268 (1.37) nm; IR ν_{max} 3363, 1706, 1600, 1508, 1452, 1048 cm^{-1}. For ^1H (600 MHz) and ^{13}C NMR (150 MHz) spectroscopic data, see Table 2. HRESIMS (negative ion) *m/z* 595.2383 $[M - H]^-$ (calcd. for $C_{29}H_{39}O_{13}$, 595.2396).

4.3.7. 4-(3′-hydroxypropenyl)-2-methoxyphenyl-1-O-β-D-{6″-O-[(1‴S,2‴R,4‴S, 6‴R,7‴E,9‴Z)-dihydrophaseic acyl]}-glucopyranoside (7)

White powder; $[\alpha]_D^{20}$ − 40.0 (*c* 0.1, MeOH); UV (MeOH) λ_{max} (log ε) 203 (0.71), 266 (0.40) nm; IR ν_{max} 3404, 1706, 1600, 1508, 1452, 1074 cm^{-1}. For ^1H (400 MHz) and ^{13}C NMR (100 MHz) spectroscopic data, see Table 2. HRESIMS (positive ion) *m/z* 629.2558 $[M + Na]^+$ (calcd. for $C_{31}H_{42}NaO_{12}$, 629.2568).

4.3.8. 2-Methoxy-4-[(1′S,2′S)-1′,2′,3′-trihydroxypropyl]-phenyl-1-O-β-D-{6″-O-[(1‴S, 2‴R,4‴S,6‴R,7‴E,9‴Z)-dihydrophaseic acyl]}-glucopyranoside (8)

White powder; $[\alpha]_D^{20}$ − 35.0 (*c* 0.1, MeOH); UV (MeOH) λ_{max} (log ε) 203 (1.60), 233 (1.21), 270 (1.24) nm; IR ν_{max} 3374, 1702, 1597, 1512, 1453, 1077 cm^{-1}. For ^1H (400 MHz) and ^{13}C NMR (100 MHz) spectroscopic data, see Table 2. HRESIMS (positive ion) *m/z* 663.2634 $[M + Na]^+$ (calcd. for $C_{31}H_{44}NaO_{14}$, 663.2623).

4.4. Alkaline hydrolysis of 6–8

Compounds **6**–**8** (30 mg each) were hydrolyzed according to a reported method (Hong et al., 2017), by individually mixing them with MeOH (2.0 mL), *N*,*N*-dimethylformamide (2.0 mL), and 1 N LiOH (2.0 mL), and stirring overnight at room temperature, respectively. Each mixture was then neutralized with 1 N HCl and extracted with *n*-BuOH three times. The *n*-BuOH extract was separated by preparative HPLC (MeOH–1% formic acid in H_2O; 30:70) to give purified hydrolysates **6a** (12 mg) and **6b** (11 mg); **7a** (10 mg) and **7b** (9 mg); and **8a** (11 mg) and **8b** (10 mg), respectively.

4.4.1. Hydrolysate of 6 (6a)

HRESIMS (positive ion) *m/z* 305.1349 $[M + Na]^+$ (calcd. for $C_{15}H_{22}NaO_5$, 305.1359). ^1H NMR (CD_3OD, 600 MHz) δ_H 7.95 (1H, d, *J* = 16.2 Hz, H-8″), 6.48 (1H, d, *J* = 16.2 Hz, H-7″), 5.73 (1H, s, H-10″), 4.08 (1H, m, H-4″), 3.77 (1H, d, *J* = 7.2 Hz, H-12″a), 3.68 (1H, d, *J* = 7.2 Hz, H-12″b), 2.04 (3H, s, H-15″), 2.03 (1H, m, H-3″*α*), 1.83 (1H, m, H-5″*α*), 1.69 (1H, m, H-3″*β*), 1.62 (1H, m, H-5″*β*), 1.11 (3H, s, H-14″), 0.89 (3H, s, H-13″). ^{13}C NMR (CD_3OD, 150 MHz) δ_C 170.3 (C-11″), 150.8 (C-9″), 134.9 (C-7″), 132.0 (C-8″), 120.1 (C-10″), 87.9 (C-2″), 83.4 (C-1″), 77.4 (C-12″), 66.1 (C-4″), 49.3 (C-6″), 46.1 (C-3″), 44.6 (C-5″), 21.3 (C-15″), 19.8 (C-14″), 16.5 (C-13″). ECD (*c*, 1.31 × 10^{-3} M, MeOH) λ_{max} ($\Delta\varepsilon$) 259 nm (−0.95). The structures of **7a** and **8a** were the same as that of **6a**.

4.4.2. Hydrolysate of 6 (6b)

ESIMS (positive ion) *m/z* 355 $[M + Na]^+$. ^1H NMR (CD_3OD, 500 MHz) δ_H 6.06 (2H, d, *J* = 1.5 Hz, H-3, 5), 4.61 (1H, d, *J* = 7.5 Hz, H-1′), 3.73 (6H, s, 2, 6-OCH_3), 3.61 (1H, dd, *J* = 12.0, 5.0 Hz, H-6′a), 3.40 (1H, m, H-6′b), 3.36 (1H, m, H-3′), 3.33 (1H, m, H-2′), 3.25 (1H, m, H-5′), 3.13 (1H, m, H-4′). ^{13}C NMR (CD_3OD, 125 MHz) δ_C 156.3 (C-4), 155.0 (C-2, 6), 129.9 (C-1), 106.5 (C-1′), 94.8 (C-3, 5), 78.5 (C-5′), 78.1 (C-3′), 76.0 (C-2′), 71.6 (C-4′), 62.9 (C-6′), 57.1 (2, 6-OCH_3).

4.4.3. Hydrolysate of 7 (7b)

HRESIMS (positive ion) *m/z* 365.1206 $[M + Na]^+$ (calcd. for $C_{16}H_{22}NaO_8$, 365.1207). ^1H NMR (CD_3OD, 400 MHz) δ_H 7.12 (1H, d, *J* = 8.0 Hz, H-6), 7.09 (1H, br s, H-3), 6.96 (1H, br d, *J* = 8.0 Hz, H-5), 6.57 (1H, d, *J* = 15.6 Hz, H-1′), 6.25 (1H, dt, *J* = 15.6, 6.0 Hz, H-2′), 4.91 (1H, d, *J* = 7.8 Hz, H-1″), 4.11 (2H, d, *J* = 6.0 Hz, H-3′), 3.88 (3H, s, 2-OCH_3), 3.87 (1H, m, H-6″a), 3.71 (1H, m, H-6″b), 3.52 (1H, m, H-3″), 3.50 (1H, m, H-5″), 3.49 (1H, m, H-2″), 3.41 (1H, m, H-4″). ^{13}C NMR (CD_3OD, 150 MHz) δ_C 151.0 (C-2), 147.9 (C-1), 133.3 (C-4), 131.0 (C-1′, 2′), 121.0 (C-5), 118.0 (C-6), 111.6 (C-3), 102.9 (C-1″), 78.4 (C-3″), 78.0 (C-5″), 75.0 (C-2″), 71.3 (C-4″), 63.8 (C-3′), 62.6 (C-6″), 56.9 (2-OCH_3).

4.4.4. Hydrolysate of 8 (8b)

HRESIMS (positive ion) *m/z* 399.1266 $[M + Na]^+$ (calcd. for $C_{16}H_{24}NaO_{10}$, 399.1262). ^1H NMR (CD_3OD, 600 MHz) δ_H 7.14 (1H, d, *J* = 8.4 Hz, H-6), 7.09 (1H, d, *J* = 1.2 Hz, H-3), 6.93 (1H, dd, *J* = 8.4, 1.2 Hz, H-5), 4.89 (1H, d, *J* = 7.8 Hz, H-1″), 4.60 (1H, d, *J* = 6.0 Hz, H-1′), 3.88 (3H, s, 2-OCH_3), 3.87 (1H, d, *J* = 12.6 Hz, H-6″a), 3.71 (1H, dd, *J* = 12.6, 4.2 Hz, H-6″b), 3.68 (1H, m, H-2′), 3.65 (1H, m, H-5″), 3.53 (1H, m, H-3″), 3.48 (1H, m, H-2″), 3.45 (1H, m, H-4″), 3.41 (2H, m, H-3′). ^{13}C NMR (pyridine-d_5, 150 MHz) δ_C 149.8 (C-2), 147.1 (C-1), 138.6 (C-4), 119.9 (C-5), 115.9 (C-6), 112.1 (C-3), 102.4 (C-1″), 78.7 (C-5″), 78.6 (C-3″), 77.6 (C-2′), 74.9 (C-2″), 74.5 (C-1′), 71.2 (C-4″), 64.3 (C-3′), 62.3 (C-6″), 55.8 (2-OCH_3).

4.5. Enzymatic hydrolysis of 4, 5, and 8b

Compound **4** (10 mg), **5** (10 mg), or **8b** (10 mg) was hydrolyzed using a previously reported method (Gu et al., 2013), by their separate incubation with snailase in sodium acetate buffer (pH 4.5) at 37 °C for 48 h. To end the enzymatic reaction, the mixture was put in a water bath at 90 °C. Thereafter, each mixture was extracted with *n*-BuOH three times to obtain a fraction containing the aglycone of **4**, **5**, or **8b**,

which was further separated by preparative HPLC (MeOH–1% formic acid in H_2O; 40:60) to give the purified hydrolysate of **4a** (3.5 mg), **5a** (3.8 mg), or **8b-1** (4.5 mg).

4.5.1. Hydrolysate of **4** (**4a**)

HRESIMS (positive ion) *m/z* 267.1568 $[M + Na]^+$ (calcd. for $C_{13}H_{24}NaO_4$, 267.1567). ^{1}H NMR (CD_3OD, 400 MHz) δ_H 5.68 (1H, dd, J = 15.7, 5.9 Hz, H-8), 5.55 (1H, d, J = 15.7 Hz, H-7), 4.29 (1H, dq, J = 6.4, 5.9 Hz, H-9), 3.91 (1H, dd, J = 3.2, 2.8 Hz, H-3), 3.64 (1H, br s, H-4), 2.23 (1H, qd, J = 7.2, 2.8 Hz, H-5), 2.00 (1H, dd, J = 15.0, 3.2 Hz, H-2α), 1.37 (1H, br d, J = 15.0 Hz, H-2β), 1.24 (3H, d, J = 6.4 Hz, H-10), 1.14 (3H, s, H-11), 1.00 (3H, d, J = 7.2 Hz, H-13), 0.86 (3H, s, H-12). ^{13}C NMR (CD_3OD, 100 MHz) δ_C 135.2 (C-8), 132.7 (C-7), 81.6 (C-6), 77.1 (C-4), 72.4 (C-3), 69.3 (C-9), 39.3 (C-1), 38.4 (C-2), 32.7 (C-5), 27.6 (C-11), 26.7 (C-12), 24.3 (C-10), 13.3 (C-13). ECD (c, 2.04 × 10^{-3} M, MeOH) λ_{max} ($\Delta\varepsilon$) 200 (– 3.63).

4.5.2. Hydrolysate of **5** (**5a**)

HRESIMS (positive ion) *m/z* 267.1564 $[M + Na]^+$ (calcd. for $C_{13}H_{24}NaO_4$, 267.1567). ^{1}H NMR (CD_3OD, 400 MHz) δ_H 5.68 (1H, dd, J = 15.7, 5.9 Hz, H-8), 5.55 (1H, d, J = 15.7 Hz, H-7), 4.29 (1H, dq, J = 6.4, 5.9 Hz, H-9), 3.91 (1H, m, H-3), 3.64 (1H, br s, H-4), 2.23 (1H, qd, J = 7.2, 2.8 Hz, H-5), 2.00 (1H, dd, J = 15.0, 3.2 Hz, H-2α), 1.37 (1H, br d, J = 15.0 Hz, H-2β), 1.24 (3H, d, J = 6.4 Hz, H-10), 1.13 (3H, s, H-11), 1.03 (3H, d, J = 7.2 Hz, H-13), 0.83 (3H, s, H-12). ^{13}C NMR (CD_3OD, 100 MHz) δ_C 135.2 (C-8), 132.7 (C-7), 81.6 (C-6), 77.1 (C-4), 72.4 (C-3), 69.4 (C-9), 39.3 (C-1), 38.4 (C-2), 32.7 (C-5), 27.6 (C-11), 26.7 (C-12), 24.3 (C-10), 13.4 (C-13). ECD (c, 1.87 × 10^{-3} M, MeOH) λ_{max} ($\Delta\varepsilon$) 200 (−3.63).

4.5.3. Hydrolysate of **8b** (**8b-1**)

$[\alpha]_D^{20}$ + 42.0 (c 0.5, MeOH) HRESIMS (positive ion) *m/z* 237.0731 $[M + Na]^+$ (calcd. for $C_{10}H_{14}NaO_5$, 237.0733). ^{1}H NMR (pyridine-d_5, 400 MHz) δ_H 7.51 (1H, br s, H-3), 7.35 (1H, br d, J = 8.0 Hz, H-5), 7.26 (1H, d, J = 8.0 Hz, H-6), 5.32 (1H, d, J = 5.6 Hz, H-1′), 4.44 (1H, m, H-2′), 4.26 (1H, dd, J = 3.6, 11.0 Hz, H-3′a), 4.12 (1H, dd, J = 6.4, 11.0 Hz, H-3′b), 3.68 (3H, s, 2-OCH_3). ^{13}C NMR (pyridine-d_5, 100 MHz) δ_C 148.8 (C-2), 147.7 (C-1), 135.7 (C-4), 120.9 (C-5), 116.5 (C-6), 112.0 (C-3), 78.3 (C-2′), 75.3 (C-1′), 64.8 (C-3′), 56.1 (2-OCH_3).

4.6. Preparation of (S)- and (R)-MTPA ester derivatives of **4a** and **5a**

A solution of **4a** (2.0 mg) in anhydrous pyridine (2 mL) was reacted with (*R*)-α-methoxy-α-trifluoromethylphenylacetyl chloride (MTPA chloride; 10 mg) in the presence of dimethylaminopyridine (30 mg) and allowed to stand at 37 °C for 10 h H_2O (1 mL) was then added and the solution was dried under vacuum. The residue was redissolved in MeOH and purified by preparative HPLC (MeOH–1% formic acid in H_2O; 65:35) to obtain the (*R*)-MTPA ester derivative of **4a** (**4a-a**) (1.8 mg) (Shu et al., 2013). (*S*)-MTPA chloride and **4a** were mixed and separated in the same manner to obtain the (*S*)-MTPA derivative of **4a** (**4a-b**) (2.3 mg). The (*R*) and (*S*)-MTPA esters of **5a** (**5a-a** and **5a-b**) were obtained from **5a** using the same procedure.

4.6.1. (R)-MTPA derivative of **4a** (**4a-a**)

^{1}H NMR (CD_3OD, 400 MHz) δ_H 5.79 (1H, d, J = 15.2 Hz, H-7), 5.72 (1H, dd, J = 15.2, 7.2 Hz, H-8), 5.60 (1H, m, H-9), 3.92 (1H, br d, J = 2.8 Hz, H-3), 3.65 (1H, br s, H-4), 2.24 (1H, qd, J = 7.2, 2.5 Hz, H-5), 2.02 (1H, dd, J = 15.0, 3.2 Hz, H-2α), 1.37 (3H, d, J = 6.0 Hz, H-10), 1.30 (1H, m, H-2β), 1.12 (3H, s, H-11), 0.99 (3H, d, J = 7.2 Hz, H-13), 0.81 (3H, s, H-12).

4.6.2. (S)-MTPA derivative of **4a** (**4a-b**)

^{1}H NMR (CD_3OD, 400 MHz) δ_H 5.60 (3H, br s, H-7, 8, 9), 3.90 (1H, br d, J = 2.8 Hz, H-3), 3.63 (1H, br s, H-4), 2.19 (1H, qd, J = 7.2, 2.5 Hz, H-5), 1.99 (1H, dd, J = 15.0, 3.2 Hz, H-2α), 1.42 (3H, d, J = 6.0 Hz, H-10), 1.29 (1H, m, H-2β), 1.04 (3H, s, H-11), 0.95 (3H, d, J = 7.2 Hz, H-13), 0.76 (3H, s, H-12).

4.6.3. (R)-MTPA derivative of **5a** (**5a-a**)

^{1}H NMR (CD_3OD, 400 MHz) δ_H 5.71 (1H, d, J = 15.2 Hz, H-7), 5.66 (1H, dd, J = 15.2, 6.8 Hz, H-8), 5.61 (1H, m, H-9), 3.91 (1H, m, H-3), 3.64 (1H, m, H-4), 2.21 (1H, m, H-5), 2.00 (1H, dd, J = 15.0, 3.2 Hz, H-2α), 1.41 (3H, d, J = 6.0 Hz, H-10), 1.31 (1H, m, H-2β), 1.07 (3H, s, H-11), 0.92 (3H, d, J = 7.2 Hz, H-13), 0.78 (3H, s, H-12).

4.6.4. (S)-MTPA derivative of **5a** (**5a-b**)

^{1}H NMR (CD_3OD, 400 MHz) δ_H 5.81 (1H, d, J = 15.2 Hz, H-7), 5.74 (1H, dd, J = 15.2, 6.8 Hz, H-8), 5.61 (1H, m, H-9), 3.92 (1H, m, H-3), 3.65 (1H, m, H-4), 2.24 (1H, m, H-5), 2.01 (1H, dd, J = 15.0, 3.2 Hz, H-2α), 1.34 (3H, d, J = 6.0 Hz, H-10), 1.32 (1H, m, H-2β), 1.11 (3H, s, H-11), 0.97 (3H, d, J = 7.2 Hz, H-13), 0.81 (3H, s, H-12).

4.7. Determination of the absolute configurations of sugar groups

The absolute configurations of the sugar groups were assigned according to a previously reported procedure (Su et al., 2018). The compounds (2.0 mg each) were hydrolyzed with 1 M HCl (1 mL) at 100 °C for 2 h, and then extracted with EtOAc (5.0 mL) three times. The H_2O layer was dried, and the residue or sugar standard was dissolved in pyridine (0.5 mL). L-Cysteine methyl ester hydrochloride (2.0 mg) was then added and heated at 60 °C for 2 h. Next, *o*-tolyl isothiocyanate (2.0 μL) was added and further heated at 60 °C for 2 h. Finally, the mixture was directly analyzed by HPLC (Agilent 1200) at 250 nm. A Cosmosil 5C18-AR-II HPLC column (150 mm × 4.6 mm i.d., 5 μm particle size; Nacalai Tesque Inc., Kyoto, Japan) at 35 °C was used to analyze each sample by isocratic elution with CH_3CN–H_2O (25:75) at a flow rate of 0.8 mL/min. The retention time of D-glucopyranose (10.4 min) was measured and compared with those of the reaction mixtures. As the sugar derivatives from the compounds showed very similar retention times to the sugar standard, the types and absolute configurations of the sugars were confirmed to be D-glucopyranose.

4.8. Croton oil-induced mouse ear edema

Kunming male mice were purchased from the Animal Center of Military Medical Science (Beijing, China). The animal experiments complied with the Institutional Guidelines for Animal Care and Use of the Chinese Academy of Medical Sciences and Peking Union Medical College. The croton oil-induced mice ear edema assay was conducted according to established methods (Tang et al., 2014). The mice were randomized and injected subcutaneously with different extracts of *S. rubriflora* leaves and twigs (1 mg/g) 1 h before croton oil application. Topical inflammation was induced on the right ear of the adult mice by injecting croton oil (0.4 mg/15 μL). The left ear received the same volume of acetone as a blank control. To evaluate the anti-inflammatory activity of *S. rubriflora*, the mice were euthanized 4 h after injection of the croton oil, and tissue punches of the treated (right) and untreated (left) ears were weighed.

4.9. Cell culture

The RAW264.7 cell line was purchased from the cell bank of the Chinese Academy of Science. Cells were cultured in RPMI-1640 (Invitrogen, Carlsbad, CA, USA) with fetal bovine serum (10%; Hyclone, Logan, UT, USA), penicillin (100 U/mL; Sigma-Aldrich), streptomycin (100 mg/mL; Sigma-Aldrich), and glutamine (4 mM; Sigma-Aldrich). Cells were seeded in plates at appropriate cell densities per well. At 80% confluency, cells were pretreated with DMSO (negative control), kaempferol (positive control) (Wall et al., 2013; Kowalski et al., 2005) or various concentrations of compounds with LPS (100 ng/mL) (Invitrogen) for 18 h, followed by RNA collection for real-time

PCR.

4.10. RNA isolation and evaluation of gene expression

Total RNAs were extracted using TRIzol reagent (MRC Inc., Cincinnati, OH, USA), followed by DNase digestion and column cleanup with Qiagen mini-columns (Valencia, CA, USA). Reverse transcription was performed with an iScript cDNA synthesis kit (Bio-Rad, Hercules, CA, USA). The following real-time PCR primers (Integrated DNA Technologies, Coralville, IA, USA) were used: GAPDHR sense (GGCCT CCAAGGAGTAAGAAA) and anti-GAPDHR sense (GCCCCTCCTGTTAT TATGG); TNF-α sense (CCCCAGTCTGTATCCTTCTAA), and TNF-α antisense (TCGAGGCTCCAGTGAATT); IL-6 sense (CCCCAATTTCCAATG CTCTCC) and IL-6 antisense (CGCACTAGGTTTGCCGAGTA). Real-time PCR was performed with SYBR Green and the 7500 Fast Sequence Detection System (Applied Biosystems, Foster City, CA, USA). All primers for real-time PCR analysis were designed using Primer Express software 2.0.0 (Applied Biosystems), and GAPDHR was used as the normalization reference.

Conflicts of interest

The authors declare no competing financial interest.

Acknowledgments

This study was supported by the CAMS Innovation Fund for Medical Sciences (CIFMS) (2016-I2M-1-010), the Fund of Jiansheng Fresh Herb Medicine Research and Drug Innovation Major Project (2018ZX09711001-008-009).

Appendix. ASupplementary data

Supplementary data to this article can be found online at https://doi.org/10.1016/j.phytochem.2019.03.021.

References

Cioffi, G., Braca, A., Autore, G., Morelli, I., Pinto, A., Venturella, F., De Tommasi, N., 2003. Cytotoxic saponins from *Schefflera fagueti*. N. Planta Med. 69, 750–756.
Comte, G., Joseph Vercauteren, G., Chulia, A.J., Allais, D.P., Delage, C., 1997. Phenylpropanoids from leaves of *Juniperus phoenicea*. Phytochemistry 45, 1679–1682.
Gaskin, P., Hutchison, M., Lewis, N., Macmillan, J., Phinney, B., 1984. Microbiological conversion of 12-oxygena and other derivatives of ent-kaur-16-en-19-oic acid by gibberella fujikuroi, mutant B1-41a. Phytochemistry 23, 559–564.
Gu, J., Li, W., Xiao, D., Wei, S., Cui, W., Chen, W., Hu, Y., Bi, X., Kim, Y., Li, J., Du, H., Zhang, M., Chen, L., 2013. Compound K, a final intestinal metabolite of ginsenosides, enhances insulin secretion in MIN6 pancreatic β-cells by upregulation of GLUT2. Fitoterapia 87, 84–88.
Hong, M., Kim, J., 2017. Determination of the absolute configuration of khellactone esters from *Peucedanun japonicum* roots. J. Nat. Prod. 80, 1354–1360.
Hu, X., Zhang, W., Zhu, Q., 1998. Zhonghua Herb (Part 15). Shanghai Science and Technology Press, Shanghai, pp. 867.
Ikuta, A., 1992. Triterpenes from *Stauntonia hexaphylla* callus tissues. J. Nat. Prod. 55, 1230–1233.
Ishikawa, T., Fujimatu, E., Kitajima, J., 2002. Water-soluble constituents of anise: new glucosides of anethole glycol and its related compounds. Chem. Pharm. Bull. 50, 1460–1466.
Kowalski, J., Samojedny, A., Paul, M., Pietsz, G., Wilczok, T., 2005. Effect of apigenin, kaempferol and resveratrol on the expression of interleukin-1β and tumor necrosis factor-α genes in J774.2 macrophages. Pharmacol. Rep. 57, 390–394.
Kong, F., Lee, B., Wei, K., 2019. 5-Hydroxymethylfurfural mitigates lipopolysaccharide-stimulated inflammation *via* suppression of MAPK, NF-κB and mTOR activation in RAW 264.7 cells. Molecules 24, 275.
Lai, H.C., Lu, C.H., Wong, C.S., Lin, B.F., Chan, S.M., Kuo, C.Y., Wu, Z.F., 2018. Baicalein attenuates neuropathic pain and improves sciatic nerve function recovery in rats with partial sciatic nerve transection. J. Chin. Med. Assoc. 81, 955–963.
Li, Y., Jiang, R., Ooi, L.S., But, P.P., Ooi, V.E., 2007. Antiviral triterpenoids from the medicinal plant *Schefflera heptaphylla*. Phytother Res. 21, 466–470.
Li, J., Yang, J., Lu, F., Qi, Y., Liu, Y., Sun, Y., Wang, Q., 2012. Chemical constituents from the stems of *Celastrus orbiculatus*. Chin. J. Nat. Med. 10, 279–283.
Liu, Y., Li, F., Zhang, L., Wu, J., Wang, Y., Yu, H., 2017. Taurine alleviates lipopolysaccharide-induced liver injury by anti-inflammation and antioxidants in ats. Mol. Med. Rep. 16, 6512–6517.
Luo, Q., Yang, A., Cao, Q., Guan, H., 2018. 3,3′-Diindolylmethane protects cardiomyocytes from LPS-induced inflammatory response and apoptosis. BMC Pharmacol Toxicol 19, 71–79.
Milborrow, B.V., 1975. The absolute configuration of phaseic and dihydrophaseic acids. Phytochemistry 14, 1045–1053.
Muir, A.D., Cole, A.L.J., Walker, J.R.L., 1982. Antibiotic compounds from New Zealand plants. I. Falcarindiol, an anti-dermatophyte agent from Schefflera digitata. Planta Med. 44, 129–133.
Nguyen, T.P., Tran, T.T.V., Mai, D.T., Le, T.D., Phan, N.M., Bui, T.D., 2015. New C_{20}-gibberellin diterpene from the leaves of *Schefflera sessiliflora* De P. V. Nat. Prod. Res. 29, 1432–1436.
Otsuka, H., Takeuchi, M., Inoshiri, S., Sato, T., Yamasaki, K., 1989. Phenolic compounds from *Coix lachrymal-jobi var.* Ma-yuen. Phytochemistry 28, 883–886.
Sang, G., Chen, Z., Shao, M., 2015. Chinese Pharmacopeia (Part 1). Beijing Xinhua Press, Beijing, pp. 812.
Seebacher, W., Simic, N., Weis, R., Saf, R., Kunert, O., 2003. Complete assignments of ^{1}H and ^{13}C NMR resonances of oleanolic acid, 18α-oleanolic acid, ursolic acid and their 11-oxo derivatives. Magn. Reson. Chem. 41, 636–638.
Shu, P., Wei, X., Xue, Y., Li, W., Zhang, J., Xiang, M., Zhang, M., Luo, Z., Li, Y., Yao, G., Zhang, Y., 2013. Wilsonols A-L, mesgastigmane sesquiterpenoids from the leaves of *Cinnamomum wilsonii*. J. Nat. Prod. 76, 1303–1312.
Su, X., Zhang, J., Li, C., Li, F., Wang, H., Gu, H., Li, B., Chen, Kang, J., 2018. Glycosides of naphthohydroquinones and anthraquinones isolated from the aerial parts of, *Morinda parvifolia*, Bartl. ex DC (Rubiaceae) increase p53 mRNA expression in A2780 cells. Phytochemistry 152, 97–104.
Takeshita, M., Yaguchi, R., Akutsu, N., 1992. Enzymatic preparation of chiral 1-phenylglycidols and 1-phenyl-1,2-propanediols. Tetrahedron Asymmetry 3, 1369–1372.
Tang, W., Xie, J., Xu, S., Lv, H., Lin, M., Yuan, S., Bai, J., Hou, Q., Yu, S., 2014. New nitric oxide-releasing derivatives of brusatol as anti-inflammatory agents: design, synthesis, biological evaluation, and nitric oxide release studies. J. Med. Chem. 57, 7600–7612.
Wall, C., Lim, R., Poljak, M., Lappas, M., 2013. Dietary flavonoids as therapeutics for preterm birth: luteolin and kaempferol suppress inflammation in human gestational tissues *in vitro*. Oxid. Med. Cell. Longev. 2013 485201.
Wang, Y., Chen, R., Yu, D., 2013. Advances of chemical constituents and pharmacological activities of *Schefflera genus*. Zhongguo Zhongyao Zazhi 38, 2254–2263.
Wang, Y., Zhang, C., Liu, Y., Liang, D., Luo, H., Hao, Z., Chen, R., Yu, D., 2014. Hepatoprotective triterpenoids and saponins of *Schefflera kwangsiensis*. Planta Med. 80, 215–222.
Wang, Y., Liu, Y., Zhang, C., Liang, D., Luo, H., Hao, Z., Chen, R., Yu, D., 2016. Four new triterpenoid saponins isolated from *Schefflera kwangsiensis* and their inhibitory activities against FBPase1. Phytochem. Lett. 15, 204–209.
Wu, C., Duan, Y., Tang, W., Li, M., Wu, X., Wang, G., Ye, W., Zhou, G., Li, Y., 2014. New ursane-type triterpenoid saponins from the stem bark of *Schefflera heptaphylla*. Fitoterapia 92, 127–132.
Wu, Z., Zhou, T., Xiao, P., 1990. Xinhua Herb (Part 3). Shanghai Science and Technology Press, Shanghai, pp. 232.
Wu, Z., Peter, R., 2007. Flora of China (Part 13). Science Press, Beijing, pp. 454.
You, R., Long, W., Lai, Z., Sha, L., Wu, K., Yu, X., Lai, Y., Ji, H., Huang, Z., Zhang, Y., 2013. Discovery of a potential anti-inflammatory agent: 3-Oxo-29-noroleana-1,9(11),12-trien-2,20-dicarbonitrile. J. Med. Chem. 56, 1984–1995.
Zhang, Z., Zhang, W., Ji, Y., Zhao, Y., Wang, C., Hu, J., 2010. Gynostemosides A-E, megastigmane glycosides from *Gynostemma pentaphyllum*. Phytochemistry 71, 693–700.
Zhou, Z., Yang, C., 2000. Chemical constituents of crude green tea, the material of *Pu-er Tea* in Yunnan. Yunnan Zhiwu Yanjiu 22, 343–350.